Clinical spectrum of MTOR-related hypomelanosis of Ito with neurodevelopmental abnormalities.

TITLE PAGE

Title

Clinical spectrum of *MTOR*-related hypomelanosis of Ito with neurodevelopmental abnormalities.

Authors

Virginie Carmignac PhD[1,2], Cyril Mignot MD PhD[3,4*], Emmanuelle Blanchard MD PhD[5,6*], Paul Kuentz MD PhD[1,7], Marie-Hélène Aubriot-Lorton MD[8], Victoria E.R. Parker PhD[9], Arthur Sorlin MD PhD[1,7,10], Sylvie Fraitag MD[11], Jean-Benoît Courcet MD[1,7,10], Yannis Duffourd MSc[1,7], Diana Rodriguez MD PhD[4], Rachel G Knox[9], Satyamaanasa Polubothu MD PhD[12,13,14], Anne Boland PharmD PhD[15], Robert Olaso PhD[15], Marc Delepine[15], Véronique Darmency MD[10], Melissa Riachi PhD[13,14], Chloé Quelin MD[16], Paul Rollier MD[16], Louise Goujon MD[16], Sarah Grotto MD[17], Yline Capri MD[17], Marie-Line Jacquemont MD[18], Sylvie Odent MD PhD[16], Daniel Amram MD[19], Martin Chevarin MSc[1,20], Catherine Vincent-Delorme MD[21], Benoît Catteau MD[22], Laurent Guibaud MD PhD[23], Alexis Arzimanoglou MD PhD[24,25], Malika Keddar[26], Catherine Sarret[27], Patrick Callier MD PhD[1,7,26], Didier Bessis MD PhD[28], David Geneviève MD PhD[29], Jean-François Deleuze PhD[15], Christel Thauvin[1,7,30], Robert K. Semple MD PhD[9,31], Christophe Philippe PhD[1,20], Jean-Baptiste Rivière PhD[1,7], Veronica A. Kinsler MD PhD[12,13,14], Laurence Faivre MD PhD[1,7,32], Pierre Vabres MD[1, 2,7]

Affiliations

[1]INSERM UMR1231, Bourgogne Franche-Comté university, Dijon, France.

[2]MAGEC-Mosaïque reference center, Dijon university hospital, Dijon France

[3] Neuropaediatrics and development pathology department, Trousseau Hospital, AP–HP, Paris, France.

[4]Genetics department and Reference Center for rare causes of Intellectual Disability, Pitié-Salpêtrière hospital, AP-HP, Paris, France.

[5] Plateforme IBiSA de Microscopie Electronique, Anatomie et cytologie pathologique, Université et CHRU de Tours, Tours, France

[6] INSERM U1259 MAVIVH, Université et CHRU de Tours, Tours, France

[7] Fédération Hospitalo-Universitaire Médecine Translationnelle et Anomalies du Développement (TRANSLAD), Dijon-Burgundy university hospital, Dijon, France.

[8] Pathology department, Dijon-Burgundy university hospital, Dijon, France.
[9] The University of Cambridge Metabolic Research Laboratories, Institute of Metabolic Science, Cambridge, United Kingdom.
[10] Pediatrics and medical genetics department, Dijon-Bourgogne university hospital, Dijon, France.
[11] Service d'Anatomie et Cytologie Pathologique, Necker-Enfants malades Hospital, Paris, France
[12] Paediatric Dermatology, Great Ormond St Hospital for Children NHS Foundation Trust, London, UK
[13] UCL GOS Institute of Child Health, London, UK
[14] Mosaicism and Precision Medicine laboratory, Francis Crick Institute, London, UK
[15] National Genotyping Center, Genomic Institute, CEA, Evry, France.
[16] Clinical Genetics department, Rennes university Hospital, Rennes, France
[17] Genetics department, AP-HP, Robert-Debré University Hospital, Paris, France
[18] Medical Genetics Unit, CHU La Réunion, Saint-Pierre, France
[19] Clinical genetics department, Créteil hospital, Créteil, France
[20] «Unité Fonctionnelle Innovation en Diagnostic Génomique des Maladies Rares, FHU-TRANSLAD, CHU Dijon Bourgogne university hospital, Dijon, France
[21] Medical genetic department, Jeanne de Flandre hospital, Lille, France.
[22] Dermatology department, Lille university hospital, Lille, France
[23] Pediatric and Fetal imaging department, Hospices Civils de Lyon, Bron, France.
[24] Department of Paediatric Clinical Epileptology, Sleep Disorders and Functional Neurology, Member of the ERN EpiCARE, University Hospitals of Lyon (HCL), Lyon, France
[25] Brain Dynamics and Cognition (DYCOG) Team, Lyon Neuroscience Research Centre, Lyon, France.
[26] Cytogenetics department, Dijon university hospital, Dijon, France.
[27] Medical genetics department, Pôle Femme et Enfant, Clermont-Ferrand university hospital- Hôpital d'Estaing, Clermont-Ferrand, France
[28] Dermatology department, Montpellier university hospital, Montpellier, France.
[29] Medical genetics department, Montpellier university hospital, Montpellier, France.
[30] Centre de Référence Déficiences Intellectuelles de Causes Rares, Hôpital d'Enfants, Dijon, France
[31] Center for Cardiovascular Science, University of Edinburgh, Edinburgh, UK

[32]Centre de Référence Anomalies du Développement et Syndromes Malformatifs, Hôpital d'Enfants, Dijon, France

Correspondence:
Virginie Carmignac,
Centre de référence MAGEC Mosaïque,
Centre Hospitalo-Universitaire Dijon Bourgogne,
15 boulevard Maréchal de Lattre de Tassigny
21070 Dijon cedex, France.
Phone: +33 3 80 39 66 58.
Fax: +33 3 80 39 66 00.
Email: virginie.carmignac@chu-dijon.fr

CONFLICT OF INTEREST

The authors state no conflict of interest.

ABSTRACT

Purpose. Hypomelanosis of Ito (HI) is a skin marker of somatic mosaicism. Mosaic *MTOR* pathogenic variants have been reported in HI with brain overgrowth. We sought to delineate further the pigmentary skin phenotype, and clinical spectrum of neurodevelopmental manifestations of *MTOR*-related HI.

Methods. From two cohorts totaling 71 patients with pigmentary mosaicism, we identified 14 patients with Blaschko-linear and one with flag-like pigmentation abnormalities, psychomotor impairment or seizures, and a postzygotic *MTOR* variant in skin. Patient records, including brain MRI were reviewed. Immunostaining (n=3) for melanocyte markers and ultrastructural studies (n=2) were performed on skin biopsies.

Results. *MTOR* variants were present in skin, but absent from blood in half of cases. In a patient (p.(Glu2419Lys) variant), phosphorylation of p70S6K was constitutively increased. In hypopigmented skin of two patients, we found a decrease in stage 4 melanosomes in melanocytes and keratinocytes. Most patients (80%) had macrocephaly or (hemi)megalencephaly on MRI.

Conclusion. *MTOR*-related HI is a recognizable neurocutaneous phenotype of patterned dyspigmentation, epilepsy, intellectual deficiency, and brain overgrowth, and a distinct subtype of hypomelanosis related to somatic mosaicism. Hypopigmentation may be due to a defect in melanogenesis, through mTORC1 activation, similar to hypochromic patches in tuberous sclerosis complex.

INTRODUCTION

Hypopigmentation along Blaschko's lines defines hypomelanosis of Ito (HI). Although in the initial description [1], extracutaneous findings were not reported, HI was later recognized as a neurocutaneous disorder, because of the frequency of brain involvement and epilepsy [2–4]. Hemihypertrophy and additional developmental anomalies also appear to be more common in HI [5,6]. In some patients, it may be difficult to determine whether the affected skin is hypopigmented or hyperpigmented [7], hence the name "pigmentary mosaicism", encompassing both types of linear dyschromia [8]. For hypopigmentation, the denominations "pigmentary mosaicism of the Ito type" or "linear hypomelanosis in narrow bands" have also been suggested [9].

The genetic basis of HI is only partially understood. It has long been recognized as a hallmark of somatic mosaicism, since multiple non-recurrent mosaic chromosomal anomalies have been reported in patients with this clinical feature[10,11]. In contrast to chromosomal anomalies however, few mosaic single-gene anomalies have been reported in pigmentary mosaicism so far. In rare cases, mosaic activating *MTOR* pathogenic variants have been detected in the brain, blood or buccal swabs (Supplementary table 1), but in most patients, genetic testing was not performed on skin biopsy, and their functional consequences on skin pigmentation were not studied.

Besides somatic mosaic *MTOR* pathogenic variants in brain tissue, germline *MTOR* pathogenic variants have been reported in patients with Smith-Kingsmore syndrome (OMIM #616638) (Supplementary Figure 1), which consists of intellectual disability with macrocephaly, ventriculomegaly, seizures and facial dysmorphism (mid-face hypoplasia, hypertelorism, downslanted palpebral fissures, depressed nasal bridge, thin upper lip, flat philtrum).

To characterize hypomelanosis of Ito with neurodevelopment anomalies related to *MTOR*

variants clinically and genetically, we performed in-depth phenotyping in HI patients harboring mosaic *MTOR* pathogenic variants in the skin, including brain magnetic resonance imaging (MRI) and microscopic and ultrastructural skin analysis. We now provide further delineation of the cutaneous and neurodevelopmental spectrum associated with *MTOR* post-zygotic pathogenic variants.

MATERIALS AND METHODS

Study subjects

Patients were ascertained by clinical geneticists or dermatologists in 10 French centers (Dijon, Lille, Montpellier, Créteil, Paris-Trousseau, Rennes, Clermont-Ferrand, Reims, Paris-Robert-Debré, La Réunion), as part of a nationwide collaborative effort for identification of genes involved in cutaneous mosaic syndromes. Inclusion in the cohort required presence of both cutaneous and extracutaneous manifestations. Inclusion criteria in the phenotype study consisted of skin or hair hypopigmentation in a mosaic pattern - linear, segmental, or flag-like - associated with any type of extracutaneous involvement, and presence of a postzygotic *MTOR* variant. Criteria of non-inclusion were diagnoses of Mendelian disorders of pigmentation, particularly Waardenburg syndrome and piebaldism, or hypochromic bands resulting from linear inflammatory conditions, such as lichen striatus or ILVEN (Inflammatory linear verrucous epidermal nevus). All clinical features were recorded on a clinical research form, and cutaneous images were centralized and reviewed at the coordination center by two experts (AS, PV). Cerebral MRI was performed at each center and centralized reading was performed by three other experts (CM, DR, LG).

Next generation sequencing

DNA analysis was performed at Dijon GAD laboratory, université de Bourgogne, for 13

patients, and at University College London for two patients. Genomic DNA was extracted from blood, 5-mm punch biopsies of hypopigmented skin, cultured skin fibroblasts, buccal swabs and saliva specimens. Details on next generation sequencing are available in **Supplementary Method**.

In-depth exome sequencing on whole skin biopsies and blood genomic DNA was initially performed in 31 patients with hypopigmented bands along Blaschko's lines or segmental hypochromic patches, associated with various extracutaneous features (Flow diagram in Supplementary Figure 2). We found a mosaic *MTOR* pathogenic variant in the skin from one patient–with–hemimegalencephaly and severe epilepsy. Other patients carried a mosaic chromosomal abnormality (7 cases), a germline X-linked variant in *TFE3* [12,13] (1 case), a postzygotic variant in *RHOA* [14] (2 cases) or other candidate genes (4 cases), or remained negative (16 cases). Targeted deep sequencing of *MTOR* was subsequently performed on hypopigmented skin and/or blood DNA from 40 additional patients with Blaschko-linear hypopigmentation associated with epilepsy or intellectual deficiency who were subsequently ascertained (Supplementary Figure 2).

Assessment of mTOR activation on cultured skin fibroblasts

Fibroblasts were obtained from a skin biopsy of patients P03 and P12. The presence of c.4556C>T (p.(Ala1519Val)) and c.7255G>A (p.(Glu2419Lys)) substitutions was checked both by Sanger sequencing (ABI BigDye Terminator Cycle Sequencing kit (v.3.1) and an ABI 3130 Genetic Analyzer, Applied Biosystems, Villebon-sur-Yvette, France), and TUDS, which allowed determination of variant allele fractions (VAFs). A mixed culture of non-mutant and *MTOR*-mutant skin fibroblasts (p.(Glu2419Lys), VAF = 40%), three wild-type control fibroblast cultures (C1, C2, C3), and mixed cultures of non-mutant and *PIK3CA*-mutant control fibroblasts (p.(Gly1049Arg), VAF = 40%), M098 (p.(Gly418Lys), VAF = 32%),

M018 (p.(Gln546Lys), VAF = 40%) and M032 (p.(His1047Arg), VAF = 30%) were studied. Cells were maintained at 37°C in a humidified incubator in DMEM supplemented with 10% FBS, 1,000 u/l penicillin, 0.1 g/l streptomycin, and 2 mmol/l L-glutamine. Amino acid deprivation procedures were conducted as previously described [15,16].

Phosphorylation of AKT at residue 473 was assessed using a direct ELISA assay kit (InstantOne®, eBioscience, Cambridge, UK, Cat No 85-86042-253). Results were expressed relative to control levels and pooled; statistical analysis was performed using one-way ANOVA with Tukey's post-hoc analyses. Phosphorylation of p70S6K at residue 389 was assessed by immunoblotting and antibody labeling by Calnexin (#2679) and p70S6Kthr389 (#9234, Cell Signalling Technology, London, UK). Cell size was measured on 10,000 cells per run on an MS3 multi-sizer (Beckmann-Coulter), after incubation of fibroblasts with or without amino acids, since phosphorylation of the PI3K-AKT-MTOR pathway depends on nutrients.

Microscopy

Additional skin biopsies for optical and electron microscopy were obtained from patients in each center and standard FFPE skin sections were processed prior to centralized analysis. Immunoperoxidase staining was performed on FFPE sections from P12 (hypopigmented and normal skin), P05 and P06 (hypopigmented skin only) and two control FFPE sections from age-matched controls, using anti-MITF (#NCL-L-MITF, 1:500, Leica, Nanterre, France) and anti-MelanA (1:200; ab731; Abcam, Cambridge, USA) mouse monoclonal antibodies. Glutaraldehyde-fixed skin biopsies from P12 and P11 were prepared for electron microscopy following standard procedures. Ultrathin sections (120 nm-thick) were observed on a JEOL JEM-1011 transmission electron microscope (JEOL, Croissy, France) operating at 100 kV and

pictures taken using ES1000W Erlangshen CCD camera (GATAN, Elancourt, France). Stage I and stage IV melanosomes were counted in 15 melanocytes from biopsies taken from both normal (control) and hypomelanotic skin from patients P12 and P11, respectively. Melanosomes were counted in 50 basal layer keratinocytes for each sample. Statistical significance of differences was assessed using Wilcoxon rank sum test, with a p-value < 0.05 considered significant.

RESULTS

In one affected individual from the initial cohort of 31 patients (P12), exome sequencing on DNA from hypopigmented skin identified a *de novo* predicted missense p.(Glu2419Lys) (c.7255G>A) *MTOR* variant, present in 21 of 74 reads (28%), absent from blood-derived DNA from her unaffected parents (Supplementary Table 2). The variant was absent from GnomAD variant database, found to affect a highly conserved nucleotide and amino acid, and was predicted as likely deleterious *in silico.* TUDS of the *MTOR* kinase domain harboring the c.7255G>A substitution confirmed its presence in 29% of alleles in whole skin biopsy, and 41% of alleles in cultured skin fibroblasts. The variant was nearly undetectable in blood (less than 1% of reads) (Figure 1).

In the second cohort of 40 patients, this variation and ten additional postzygotic *MTOR* substitutions were identified in 14 unrelated patients (35.0%): p.(Lys1452Asn), p.(Cys1483Tyr), p.(Ala1519Val), p.(Ala1519Thr), p.(Glu1799Lys), p.(Thr1977Ile), p.(Ile2017Thr), p.(Ser2413Ile), p.(Leu2427Pro) and p.(Ile2501Phe). Hypomelanotic skin samples were available for further study in 13/15 individuals with mosaic *MTOR* variants, and normally pigmented skin DNA was also available in one patient (P02). Skin variant allele fractions (VAFs) varied between 10% and 40% (median = 21%). Blood samples were

available in 12/15 individuals. *MTOR* variants were found in blood in 6/12 patients, with lower VAFs than in the skin, between 1% and 30% (median = 0%) (Figure 1, Supplementary Table 3). Recurrent *MTOR* hotspots were identified in nine patients: p.(Glu1799Lys), p.(Glu2419Lys), and p.(Ala1519Thr)/p.(Ala1519Val) in two patients, as well as p.(Thr1977Ile) in three patients. Overall, five variants (p.(Lys1452Asn), p.(Ala1519Thr), p.(Ala1519Val), p.(Ile2017Thr), p.(Ser2413Ile)) had never been reported previously.

Both p.(Glu2419Lys) and p.(Ile2017Thr) *MTOR* variants were previously found to result in constitutive mTOR complex 1 (mTORC1) activity *in vitro* and *in vivo* [17,18]. Primary skin fibroblasts from P12, with a variant allele fraction of 40%, were used to test p.(Glu2419Lys) mTOR activity by assessing AKT and p70 ribosomal protein S6 kinase (p70S6K) phosphorylation status [15,19] (Supplementary Figure 3). ELISA (Supplementary Figure 3a) and immunoblotting experiments (Supplementary Figure 3b) following amino acid deprivation showed increased levels of phosphorylated AKT^{ser473} and $p70S6K^{thr389}$ in mutant cells as compared to controls. AKT^{ser473} and $p70S6K^{thr389}$ phosphorylation levels were similar to those of skin fibroblasts harboring *PIK3CA* activating variants (Supplementary Figure 3). However, in amino acid-rich conditions, the p.(Glu2419Lys) *MTOR* mutant cells showed no constitutive activity, in contrast with *PIK3CA* mutant cell lines (Supplementary Figure 3c). We found no significant differences in median cell diameter between mutant and control cells (Supplementary Figure 3d). In comparison, in primary cultured fibroblasts harboring the p.(Ala1519Val) *MTOR* variant at very low levels (< 1%), phosphorylation was not increased at baseline or under amino acid deprivation.

The 15 patients (10 females and 5 males) aged 1 - 30 years (median: 6 years), consisted of 13 children aged 14 or younger and two adults. Fourteen patients had either well-limited or ill-

defined linear hypopigmentation along Blaschko's lines, in a typical S-shaped, V-shaped or whorled pattern, more visible under Wood's light, mainly located on the trunk and lower limbs, without lateral predominance (Figure 2, Supplementary Table 4). One additional patient did not have linear hypomelanosis, but instead a hypopigmented patch of scalp hair, a segmental cutaneous flag-like hypopigmented patch on his shoulder, and iris heterochromia. Woolly/curly hair was found in four patients, but no other anomalies of the integument or mucous membranes were noted. Since a decrease in melanocyte numbers and melanosome maturation has been reported in ash-leaf macules of tuberous sclerosis patients harboring loss-of-function variants in *TSC1* or *TSC2*, which encode upstream inhibitors of mTOR, we studied melanogenesis in patients with *MTOR*-related HI. Biopsies from hypomelanotic and normally pigmented skin in patients P05, P06, P11 and P12, showed fewer normal melanocytes per standardized field on Melan-A immunostaining as compared to controls (mean=15.8 melanocytes/field for control skins and mean=5.2 melanocytes/field in HI skins, $p=2.6.10^{-9}$) (Figure 3). On hypomelanotic skin biopsies, MITF expression appeared normal, since anti-MITF labeling in epidermal melanocytes was unchanged (Figure 3). MITF labeling was either positive (P12) or absent (P05 and P06). We failed to identify downregulation of MITF in primary skin fibroblasts from one patient (data not shown).

In patients P12 and P11, the number of stage IV melanosomes were markedly decreased in 15 melanocytes from hypomelanotic skin (n=378 and n=282, respectively), as compared with 15 melanocytes from normal skin (n=577 and n=362, respectively) (p=0.03 for P12 and p=0.0002 for P11) (Figure 4). Likewise, the stage IV/stage I melanosome ratio in melanocytes from hypomelanotic skin was reduced by 61.9% as compared to normal skin in patient P12, and by 87.3% in patient P11. Mean numbers of melanosomes per cell were also decreased in keratinocytes from hypomelanotic skin as compared with normal skin: by 75.0% in patient

P12, and by 67.6% in patient P11 (p-value=$8.2.10^{-16}$ and $3.8.10^{-15}$ for P12 and P11).

Twelve patients had psychomotor impairment ranging from mild (first steps achieved at 20 months) to severe (sitting position achieved at 6 years). All of them subsequently had intellectual deficiency (ID). Autism spectrum disorder was present in four patients, who also had ID. Eight patients had macrocephaly (OFC $\geq$ +3 SD), associated with unilateral body overgrowth in four of them. One patient had slightly elevated OFC (+2.5 SD). Six patients had normal OFC, one of them with hemihypertrophy, (Figure 5, Supplementary Table 4). Seizures were diagnosed in 10 patients, including two without ID (Figure 5, Supplementary Table 4). Among patients with seizures, only 5 had macrocephaly, whereas all 5 patients without epilepsy had macrocephaly.

Brain MRI was performed in 10 patients: three with normal OFC and seven with macrocephaly. Among patients with macrocephaly, MRI showed normal symmetric brains without megalencephaly (normal lateral ventricles and pericerebral spaces) in four (Supplementary Table 4, Figure 2). Among the 10 patients who had seizures, MRI was performed in six and showed HMEG in all of them, either with normal OFC (<+3 SD, in three patients) or macrocephaly (OFC between +3 and +4 SD, in the three others). All six cases of HMEG were characterized on MRI by i) increased volume of the white matter, ii) absence of signal change – except in one case with bilateral frontal grey matter heterotopia – and iii) cortex thickening in two patients. HMEG was also associated with homolateral (four patients) or bilateral (one patient) narrowing of lateral ventricle frontal horns, homolateral enlargement of the thalamus and caudate nucleus (one patient), or homolateral enlargement of cerebellum hemispheres (four patients). In the five patients without epilepsy, MRI was performed in four and showed either megalencephaly (MEG) (2 cases) or normal brain (2 cases). Overall, 12

patients in our series (80%) had either macrocephaly or HMEG/MEG.

Facial dysmorphism (Figure 5, Supplementary Table 4) consisted of hypertelorism, prominent forehead, depressed nasal bridge, or downslanting palpebral fissures. In addition to iris heterochromia in two cases, ocular involvement consisted of strabismus/amblyopia, astigmatism, myopia, hypermetropia, coloboma or retinitis pigmentosa. Renal anomalies usually found in TSC (angiomyolipomas and renal cysts) were absent in patients with mosaic *MTOR* pathogenic variants. On ultrasonography, 2/12 patients had increased renal cortex echogenicity, a non-specific finding.

DISCUSSION

In this group of 71 patients with patterned dyspigmentation, we identified a subset due to mosaicism for MTOR pathogenic variants. We have further delineated the clinical spectrum of *MTOR*-related hypomelanosis of Ito with neurodevelopmental anomalies (Supplementary Table 4). These features include intellectual deficiency, macrocephaly, hemimegalencephaly, epilepsy, in addition with a pigmentation pattern suggestive of mosaicism. This combination of neurocutaneous features has previously been reported (Supplementary Table 5) in seven patients with postzygotic *MTOR* activating pathogenic variants (Supplementary Table 1). Two reported siblings with a germline *MTOR* activating variant had a pigmentary phenotype without further description [20].

The severity of neurodevelopmental phenotypes varied greatly among our patients. Intellectual functioning ranged from normal to severe ID. Patients without ID had epilepsy or megalencephaly. This neurodevelopmental spectrum overlaps with Smith-Kingsmore syndrome (SKS), caused either by germline *MTOR* pathogenic variants, or mosaic *MTOR*

pathogenic variants with high VAFs in the brain [20]. Presence of HI, absent in SKS patients with a constitutional heterozygous *MTOR* pathogenic variant, maybe an indication of mosaicism and the need for further studies. To date, intellectual disability (ID) has been reported in all patients with SKS or postzygotic *MTOR* pathogenic variants and HMEG. Severe ID was present in patient P15, who harbored a postzygotic p.(Ile2501Phe) change. In contrast, two individuals from one previously published family, who carried a germline p.(Ile2501Val) variant, had normal cognition, focal epilepsy and normal OFC [21]. Since discrepancies in the cerebral phenotype for an identical germline variant cannot be explained by different amounts of mutant brain cells, the very mild phenotype in this family would be better explained by a milder gain-of-function effect of the p.(Ile2501Val) substitution than of the p.(Ile2501Phe) substitution that we found in a mosaic state in our patient.

MRI showed HMEG in all six cases with seizures, whereas in four patients without epilepsy, MRI showed either megalencephaly (MEG) or a normal brain. This suggests that, in patients with postzygotic *MTOR* pathogenic variants, HMEG might be more epileptogenic than MEG. MRI did not show cortical or other cerebral malformations in the two MEG patients and in three of the HMEG patients, while only three patients with HMEG had focal cortex thickening suggestive of polymicrogyria or periventricular heterotopia. Hence, our series also supports that, in patients with a neurodevelopmental phenotype, HMEG or MEG without apparent brain malformation might be more suggestive of pathogenic variants in *MTOR* rather than in *PIK3CA* or *AKT3*, as previously outlined [22–25]. Interestingly, the structure and function of homogeneously enlarged brains with postzygotic *MTOR* pathogenic variants may be less altered than of those with HMEG. Indeed, previous studies comparing phenotypes related to either postzygotic or germline *MTOR* pathogenic variants have suggested that severity of neurodevelopmental impairment does not correlate with the proportion of affected brain cells

[20,21,25]. This is likely explained by increased strength of the gain-of-function effect of mosaic pathogenic variants, which would result in embryonic lethality in the germline state, as compared with a milder effect of germline pathogenic variants, which would be compatible with fetus survival.

A pigmentary phenotype with hypopigmentation and hyperpigmentation has previously been reported in one of two sibs who both harbored a germline p.(Phe2202Cys) *MTOR* variant [20], but its precise clinical description is missing, and no conclusions can be drawn from this case about the role of germline *MTOR* pathogenic variants on skin pigmentation. All patients in our series carried postzygotic *MTOR* pathogenic variants in their skin, which were absent from blood in 50% of cases tested. Linear hypopigmentation has been considered a non-specific manifestation of mosaicism, as various types of non-recurrent chromosome anomalies were initially reported in association with the phenotype, and some authors have even suggested that the term hypomelanosis of Ito should be abandoned [11]. However, we and others have now found mosaic single gene defects in HI, such as *MTOR* or *RHOA* pathogenic variants [14]. In one case of the phenotypic "opposite" of HI, linear and whorled nevoid hypermelanosis [26], where Blaschko-linear hyperpigmentation is the cardinal cutaneous feature, we have also described a pathogenic mosaic variant in the *KITLG* gene [27]. Hence, hypo/hyperpigmentation along Blaschko's lines should no longer be considered merely as a clinical marker of somatic mosaicism, since, in combination with extracutaneous findings, it may also specifically point at the causative gene.

The *MTOR* gene encodes the mechanistic target of rapamycin (mTOR). This serine-threonine kinase is highly conserved, and is an essential component of MTORC1 and MTORC2 complexes. The PI3K-AKT-mTOR signaling pathway is pivotal in cell growth, protein synthesis, autophagy, and cytoskeletal dynamics [28–30]. Although MITF labeling studies were

inconclusive, cutaneous hypopigmentation may directly result from mTOR complex hyperactivation. In tuberous sclerosis complex (TSC), a condition resulting from loss of function of *TSC1* or *TSC2* [31], activation of mTOR has been shown to suppress melanogenesis via MITF downregulation, resulting in typical ash-leaf or confetti-like hypopigmented macules [32–34]. Repigmentation can be obtained by treatment with topical mTOR inhibitor rapamycin [35], since mTORC1 inhibition results in induction of melanogenesis through upregulation of MITF and its downstream targets TRP1 and TRP2 [32,33,36,37]. In hypopigmented skin of four patients with *MTOR*-related HI, we found a decrease in melanocytes, a defect in the maturation process of melanosomes, and a reduced number of melanosomes in keratinocytes, as well as activating *MTOR* variants and increased AKT and p70S6K phosphorylation in dermal fibroblasts from patients. Our findings are consistent with upregulation of mTORC1 resulting in partial suppression of melanogenesis. Paradoxically though, in P02, normally pigmented skin harbored a VAF of 25%, whereas the VAF was only 10% in hypopigmented skin. We hypothesize that lower VAFs may result from death of mutant cells in hypopigmented areas through autophagy, as recently shown in TSC [33]. A decreased number of melanocytes was found both in hypopigmented and normal skin in P12 (Figure 3), which supports this hypothesis.

Our results highlight the diagnostic importance of accurate clinical phenotyping of mosaic syndromes, and provide further evidence that genetic defects underlying hypomelanosis of Ito extend beyond chromosomal mosaicism. Additional genetic defects remain to be identified in a number of patients with linear hypopigmentation and various associated manifestations. Yet, identification of mosaic *MTOR* pathogenic variants in hypomelanosis of Ito with neurodevelopmental defects defines a clinically- and genetically-recognizable condition. It has direct clinical implications for genetic tests and genetic counselling.

Most *MTOR* pathogenic variants, not found in the germline state, are thought to be embryonic lethal. Hence, the risk of transmission from a mosaic patient harboring this type of variant appears low or absent. However, transmission of non-lethal pathogenic variants, resulting in offspring with Smith-Kingsmore syndrome, is still possible. Although the positive predictive value of HI with neurodevelopmental anomalies for the diagnosis of *MTOR* somatic mosaicism is not yet known, in our series, *MTOR* pathogenic variants were found in more than one third (36.6%) of patients with HI and seizures. Likewise, macrocephaly and/or HMEG/MEG, found in 80% of cases in our series, appear as fairly specific, as they were absent from patients with mosaic *RHOA* pathogenic variants [14,38]. Hence, in our opinion, such typical clinical presentation warrants *MTOR* sequencing by ultra-sensitive methods. DNA from the skin or other affected tissue is required for genetic testing, since the VAF is higher in skin (21%) as compared with blood (0%), where *MTOR* pathogenic variants are usually absent or at very low levels, close to NGS detection limit (1% at a depth of 1000X). Last, clinical consequences of mTORC1 upregulation, particularly neurological involvement, may be amenable to tailored treatment with mTOR inhibitors, although data on efficacy are inconclusive so far [39].

List of investigators of the PHRC National Mosaïque

The following investigators diagnosed and ascertained patients within the scope of the PHRC National Mosaïque: Ludovic Martin[1] (non-author contributor), Frédéric Caux[2] (non-author contributor), Eve Puzenat[3] (non-author contributor), Didier Lacombe[4] (non-author contributor), Alain Taieb[5] (non-author contributor), Christine Leaute-Labreze[6] (non-author contributor), Pierre Vabres[7,8,9] (author), Laurence Faivre[7,9,10] (author), Marc Bardou[11] (non-author contributor), Christel Thauvin-Robinet[7,9,12] (author), Sylvie Manouvrier[13] (non-author contributor), Patrick Edery[14] (non-author contributor), Alice Phan[15] (non-author contributor), Sabine Sigaudy[16] (non-author contributor), Didier Bessis[17] (author), David Geneviève[18] (author), Julie Le Blay[17] (non-author contributor), Anne-Claire Bursztejn[19] (non-author contributor), Sébastien Barbarot[20] (non-author contributor), Christine Bodemer[21] (non-author contributor), Valérie Cormier-Daire[22] (non-author contributor), Christine Chiaverini[23] (non-author contributor), Catherine Eschard[24] (non-author contributor), Sylvie Odent[25] (author), Emmanuelle Bourrat-Remy[26] (non-author contributor), Alain Verloes[27] (non-author contributor), Dan Lipsker[28] (non-author contributor), Juliette Mazereeuw-Hautier[29] (non-author contributor), Annabel Maruani[30] (non-author contributor), Anne-Marie Guerrot[31] (non-author contributor), and Sophie Duvert-Lehembre[32] (non-author contributor).

1. Department of Dermatology, University Hospital Center of Angers, Angers, France.
2. Department of Dermatology, Avicenne Hospital, University Paris 13, Bobigny, France.
3. Department of Dermatology, University of Bourgogne-Franche Comté, Besançon, France
4. Medical Genetics Department, Inserm U1211, Reference Center AD SOOR, AnDDI-RARE, Bordeaux University, Centre Hospitalier Universitaire de Bordeaux, Bordeaux, France.
5. Department of Dermatology and Pediatric Dermatology, Hôpital St André, Bordeaux, France.
6. Department of Dematology, Pellegrin Children's Hospital, Bordeaux, France
7. INSERM UMR1231, Bourgogne Franche-Comté university, Dijon, France.
8. MAGEC-Mosaïque reference center, Dijon university hospital, Dijon France
9. Fédération Hospitalo-Universitaire Médecine Translationnelle et Anomalies du Développement (TRANSLAD), Dijon-Burgundy university hospital, Dijon, France.
10. Centre de Référence Anomalies du Développement et Syndromes Malformatifs, Hôpital d'Enfants, Dijon, France
11. Centre d'Investigation Clinique INSERM 1432, Centre Hospitalier Universitaire de Dijon, Dijon, Bourgogne, France.
12. Centre de Référence Déficiences Intellectuelles de Causes Rares, Hôpital d'Enfants, Dijon, France
13. Centre de référence maladies rares pour les anomalies du développement Nord-Ouest, Clinique de Génétique médicale, CHU de Lille et EA7364, Université de Lille, Lille, France.
14. Genetics department, GH Est, Hospices Civils de Lyon, Lyon, France ; GENDEV Team, CRNL, CNRS UMR 5292, INSERM U1028; Claude Bernard Lyon I University, Lyon, France.
15. Department of Dermatology, Claude Bernard-Lyon 1 University and Hospices Civils de Lyon, Lyon, France.
16. Hôpital de la Timone, Medical Genetics, Marseille, Provence-Alpes-Côte d'Azur, France ; Hôpital de la Timone, Prenatal diagnosis, Marseille, Provence-Alpes-Côte d'Azur, France.
17. Dermatology department, Montpellier university hospital, Montpellier, France.
18. Medical genetics department, Montpellier university hospital, Montpellier, France.
19. Department of Dermatology, Nancy University Hospital, Nancy, France.
20. Service de Dermatologie, Hôtel Dieu, CHU de Nantes, France.
21. Department of Dermatology, Necker Hospital des Enfants Malades, University Paris-Centre APHP 5,

Paris, France.
22. Université Paris Descartes, Sorbonne Paris Cité, Paris, France ; UMR-1163 Institut Imagine, Hôpital Necker-Enfants Malades, AP-HP, Paris, France ; Service de Génétique Médicale, Hôpital Necker-Enfants Malades, AP-HP, Paris, France.
23. Department of Dermatology, Nice University Hospital, Nice, France.
24. Department of Dermatology, Robert-Debré Hospital, Reims, France.
25. Clinical Genetics department, Rennes university Hospital, Rennes, France
26. Department of Dermatology, Reference Center for Genodermatoses and Rare Skin Diseases (MAGEC), Paris, France.
27. Service de génétique médicale, AP-HP Robert-Debré, Paris, France.
28. Clinique Dermatologique, Hôpitaux Universitaires et Université de Strasbourg, Strasbourg, France.
29. Reference Centre for Rare Skin Diseases, Dermatology Department, Larrey Hospital, Toulouse, France.
30. Department of Dermatology, Tours University Hospital, Tours, France.
31. Department of Genetics, Rouen University Hospital, Normandy Centre for Genomic and Personalized Medicine, 76821 Rouen, France.
32. Department of Dermatology, Rouen University Hospital and INSERM U1234, Centre de référence des maladies bulleuses autoimmunes, Normandie University, Rouen, France.

DATA AVAILABILITY

All *MTOR* pathogenic variants identified were submitted to the CLINVAR database under the number SUB8228199 and data are available at this URL https://www.ncbi.nlm.nih.gov/clinvar/?term=SUB8228199 .

CRediT:

Conceptualization: VC, PV; Funding acquisition: PV, JBR, VAK; Investigation: VC, CM, EB, PK, MHEL, VERP, AS, SF, JBC, DR, RGK, SP, VD, CQ, PR, LG, SG, YC, MLJ, SO, DA, CVB BC, LG, AA, CS, DB, DG, VAK, PV; Methodology: VC, CM, PV; Resources: YD, AB, RO, MD, JFD; Software: YD; Supervision: PV; Validation: MR, MC, MK, PC, CP; Writing – original draft: VC, JBR, PV; Writing – review & editing: VC, CT, RKS, VAK, LF, PV.

ACKNOWLEDGMENTS

We wish to thank the subjects and families involved in the study, the Centre National de Génotypage (CNG, Evry, France) for the exome sequencing experiments, the University of Burgundy Centre de Calcul (CCuB) for technical support and management of the informatics platform, the Centre de Ressources Biologiques (CRB) Ferdinand Cabanne for collection and conservation of skin fibroblasts. We would like to thank the Exome Aggregation Consortium

and the groups that provided exome variant data for comparison. A full list of contributing groups can be found at http://exac.broadinstitute.org/about/.

This work was funded by the Agence Nationale de la Recherche (ANR-13-PDOC-0029 to J.-B.R), the Groupe Interrégional de Recherche Clinique et d'Innovation (GIRCI) Est (to J.-B.R), the Programme Hospitalier de Recherche Clinique (PHRC) National (to P.V.), and the Société Française de Dermatologie (to P.V.). R.K.S. and V.E.R.P. are supported by the Wellcome Trust (Senior Research Fellowship in Clinical Science 210752/Z/18/Z and Clinical Research Training Fellowship 097721/Z/11/Z, respectively), and R.K.S., V.E.R.P. and R.G.K. are supported by the UK National Institute for Health Research (NIHR) Cambridge Biomedical Research Centre, and by the UK Medical Research Council Centre for Obesity and Related Metabolic Diseases. V.E.R.P. is supported by the Sackler fund. VAK was funded by the Wellcome Trust, grant number WT104076MA, and SP by the Newlife Foundation, and supported by the UK NIHR GOSH/ICH biomedical research centre.

Ethics declaration

A total of 69 individuals with pigmentary mosaicism were included in the *Mosaic Undiagnosed Skin Traits And Related Disorders* (M.U.S.T.A.R.D. - NCT01950975) cohort, approved by our regional institutional review board and ethics committee (*Comité de Protection des Personnes (CPP) EST I (Dijon)*). Two additional patients were ascertained by pediatric dermatologists from one British center at Great Ormond Street Hospital, London after approval by the London Bloomsbury Research Ethics Committee. (total = 71 individuals). Informed written consent was obtained from all subjects and participating family members, including consent to publish pictures for individuals P09, P11 and P12.

REFERENCES

1. Ito M. *Incontinentia Pigmenti Achromians. A Singular Case of Nevus Depigmentosus Systematicus Bilateralis.* Vol 55(Supplement). Tohoku J Exp Med.; 1952.

2. Schwartz MF, Esterly NB, Fretzin DF, Pergament E, Rozenfeld IH. Hypomelanosis of Ito (incontinentia pigmenti achromians): A neurocutaneous syndrome. *The Journal of Pediatrics*. 1977;90(2):236-240.

3. Hamada K, Tanaka T, Ohdo S, Hayakawa K, Kikuchi I, Katsuya H. Incontinentia pigmenti achromians as part of a neurocutaneous syndrome: A case report. *Brain and Development*. 1979;1(4):313-317.

4. Pavone P, Praticò AD, Ruggieri M, Falsaperla R. Hypomelanosis of Ito: a round on the frequency and type of epileptic complications. *Neurological Sciences*. 2015;36(7):1173-1180.

5. Glover MT, Brett EM, Atherton DJ. Hypomelanosis of ito: Spectrum of the disease. *The Journal of Pediatrics*. 1989;115(1):75-80.

6. Pascual-Castroviejo I, Roche C, Martinez-Bermejo A, et al. Hypomelanosis of ITO. A study of 76 infantile cases. *Brain and Development*. 1998;20(1):36-43.

7. Nehal KS, PeBenito R, Orlow SJ. Analysis of 54 cases of hypopigmentation and hyperpigmentation along the lines of Blaschko. *Arch Dermatol*. 1996;132(10):1167-1170.

8. Kromann AB, Ousager LB, Ali IKM, Aydemir N, Bygum A. Pigmentary mosaicism: a review of original literature and recommendations for future handling. *Orphanet J Rare Dis*. 2018;13.

9. Happle R. Mosaicism in human skin: Understanding nevi, nevoid skin disorders, and cutaneous neoplasia. *Springer-Verlag*. 2014.

10. Thomas IT, Frias JL, Cantu ES, Lafer CZ, Flannery DB, Graham JG. Association of pigmentary anomalies with chromosomal and genetic mosaicism and chimerism. *Am J Hum Genet*. 1989;45(2):193-205.

11. Sybert VP. Hypomelanosis of Ito: A Description, Not a Diagnosis. *Journal of Investigative Dermatology*. 1994;103(5, Supplement):S141-S143.

12. Villegas F, Lehalle D, Mayer D, et al. Lysosomal Signaling Licenses Embryonic Stem Cell Differentiation via Inactivation of Tfe3. *Cell Stem Cell*. 2019;24(2):257-270.e8.

13. Lehalle D, Vabres P, Sorlin A, et al. *De novo* mutations in the X-linked *TFE3* gene cause intellectual disability with pigmentary mosaicism and storage disorder-like features. *J Med Genet*. Published online May 14, 2020:jmedgenet-2019-106508.

14. Vabres P, Sorlin A, Kholmanskikh SS, et al. Post-zygotic inactivating mutations of RHOA cause a mosaic neuroectodermal syndrome. *Nature Genetics*. Published online 2019.

15. Lindhurst MJ, Parker VE, Payne F, et al. Mosaic Overgrowth with Fibroadipose Hyperplasia is Caused by Somatic Activating Mutations in PIK3CA. *Nat Genet*. 2012;44(8):928-933.

16. Bar-Peled L, Chantranupong L, Cherniack AD, et al. A tumor suppressor complex with GAP activity for the Rag GTPases that signal amino acid sufficiency to mTORC1. *Science*. 2013;340(6136):1100-1106.

17. Urano J, Sato T, Matsuo T, Otsubo Y, Yamamoto M, Tamanoi F. Point mutations in TOR confer Rheb-independent growth in fission yeast and nutrient-independent mammalian TOR signaling in mammalian cells. *Proc Natl Acad Sci U S A*. 2007;104(9):3514-3519.

18. Wagle N, Grabiner BC, Van Allen EM, et al. Activating mTOR mutations in a patient with an extraordinary response on a phase I trial of everolimus and pazopanib. *Cancer Discov*. 2014;4(5):546-553.

19. Keppler-Noreuil KM, Rios JJ, Parker VER, et al. PIK3CA-Related Overgrowth Spectrum (PROS): Diagnostic and Testing Eligibility Criteria, Differential Diagnosis, and Evaluation. *Am J Med Genet A*. 2015;0(2):287-295.

20. Gordo G, Tenorio J, Arias P, et al. mTOR mutations in Smith-Kingsmore syndrome: Four additional patients and a review. *Clinical Genetics*. 2018;93(4):762-775.

21. Møller RS, Weckhuysen S, Chipaux M, et al. Germline and somatic mutations in the MTOR gene in focal cortical dysplasia and epilepsy. *Neurol Genet*. 2016;2(6):e118.

22. Lee JH, Huynh M, Silhavy JL, et al. De novo somatic mutations in components of the PI3K-AKT3-mTOR pathway cause hemimegalencephaly. *Nat Genet*. 2012;44(8):941-945.

23. Poduri A, Evrony GD, Cai X, et al. Somatic Activation of AKT3 Causes Hemispheric Developmental Brain Malformations. *Neuron*. 2012;74(1):41-48.

24. Rivière J-B, Mirzaa GM, O'Roak BJ, et al. De novo germline and postzygotic mutations in AKT3, PIK3R2 and PIK3CA cause a spectrum of related megalencephaly syndromes. *Nat Genet*. 2012;44(8):934-940.

25. Dobyns WB, Mirzaa GM. Megalencephaly syndromes associated with mutations of core components of the PI3K-AKT-MTOR pathway: PIK3CA, PIK3R2, AKT3, and MTOR. *Am J Med Genet C Semin Med Genet*. 2019;181(4):582-590.

26. Kalter DC, Atherton DJ. Linear and whorled nevoid hypermelanosis. 1988;19(6):8.

27. Sorlin A, Maruani A, Aubriot-Lorton M-H, et al. Mosaicism for a KITLG Mutation in Linear and Whorled Nevoid Hypermelanosis. *Journal of Investigative Dermatology*. 2017;137(7):1575-1578.

28. Jacinto E, Loewith R, Schmidt A, et al. Mammalian TOR complex 2 controls the actin cytoskeleton and is rapamycin insensitive. *Nature Cell Biology*. 2004;6(11):1122-1128.

29. Zoncu R, Sabatini DM, Efeyan A. mTOR: from growth signal integration to cancer, diabetes and ageing. *Nat Rev Mol Cell Biol*. 2011;12(1):21-35.

30. Thoreen CC, Chantranupong L, Keys HR, Wang T, Gray NS, Sabatini DM. A unifying model for mTORC1-mediated regulation of mRNA translation. *Nature*. 2012;485(7396):109-113.

31. Józwiak J, Galus R. Molecular Implications of Skin Lesions in Tuberous Sclerosis. *The American Journal of Dermatopathology*. 2008;30(3):256.

32. Jeong H-S, Lee SH, Yun H-Y, et al. Involvement of mTOR signaling in sphingosylphosphorylcholine-induced hypopigmentation effects. *J Biomed Sci*. 2011;18(1):55.

33. Yang F, Yang L, Wataya-Kaneda M, et al. Dysregulation of autophagy in melanocytes contributes to hypopigmented macules in tuberous sclerosis complex. *Journal of Dermatological Science*. 2018;89(2):155-164.

34. Yang F, Yang L, Wataya-Kaneda M, Yoshimura T, Tanemura A, Katayama I. Uncoupling of ER/Mitochondrial Oxidative Stress in mTORC1 Hyperactivation-Associated Skin Hypopigmentation. *Journal of Investigative Dermatology*. 2018;138(3):669-678.

35. Wataya-Kaneda M, Tanaka M, Yang L, et al. Clinical and Histologic Analysis of the Efficacy of Topical Rapamycin Therapy Against Hypomelanotic Macules in Tuberous Sclerosis Complex. *JAMA Dermatol*. 2015;151(7):722-730.

36. Ohguchi K, Banno Y, Nakagawa Y, Akao Y, Nozawa Y. Negative regulation of melanogenesis by phospholipase D1 through mTOR/p70 S6 kinase 1 signaling in mouse B16 melanoma cells. *Journal of Cellular Physiology*. 2005;205(3):444-451.

37. Cao J, Tyburczy ME, Moss J, Darling TN, Widlund HR, Kwiatkowski DJ. Tuberous sclerosis complex inactivation disrupts melanogenesis via mTORC1 activation. *J Clin Invest*. 2017;127(1):349-364.

38. Yigit G, Saida K, DeMarzo D, et al. The recurrent postzygotic pathogenic variant p.Glu47Lys in RHOA causes a novel recognizable neuroectodermal phenotype. *Hum Mutat*. 2020;41(3):591-599.

39. Hadouiri N, Darmency V, Guibaud L, et al. Compassionate use of everolimus for refractory epilepsy in a patient with MTOR mosaic mutation. *European Journal of Medical Genetics*. 2020;63(11):104036.

.

FIGURE LEGENDS

Figure 1. Distribution of post-zygotic missense *MTOR* variations. (a) Structure of mTOR protein including the HEAT (Huntingtin, Elongation factor 3, protein phosphatase 2A, and TOR1) repeat; FAT (FRAP, ATM and TRRAP) domain; FRB (FKBP12-rapamycin binding) domain; Kinase (serine-threonine kinase kinase) domain; FATC (FAT, FRAP, ATM and TRRAP carboxy-terminal) domain; and FIT (Found in TOR) domain. VAFs (%) are shown as pie charts with a maximum allele fraction of 50%. DS: Dark skin; LS: Light skin; B (red): blood. Variation details are summarized in Supplementary Table 3. (b) Distribution of VAFs in hypopigmented skin (LS, black dots) and blood (red dots), with median values.

Figure 2. Left: Clinical pigmentary skin phenotype in two patients. (a, b) P11. **(a)** Unilateral linear and whorled hypopigmentation in multiple large bands with ragged border and sharp midline limitation on the abdomen. **(b)** Enhanced contrast on Wood's lamp illumination. **(c,d)** P12. **(c)** Linear hypopigmentation in large bands on left lower limb. **(d)** Enhanced contrast on Wood's lamp illumination. **(e, f)** Facial features of patients P09 and P11. **Right: Brain MRI of subjects P01, P03, P10 and P12. a-c:** P12. Left HMEG with altered ventricle shape (small frontal horn), enlarged left thalamus and caudate nucleus **(a)**, slightly thickened cortical mantle and enlarged white matter with normal signal **(b)** and enlarged anterior corpus callosum **(c)**. **d-f:** P03. Normal corpus callosum **(d)**, small frontal horns **(e, f)**, and mild overgrowth of the right cerebral hemisphere, with slight enlargement of the right posterior ventricle **(c)**. **g-i:** P10. Normal corpus callosum on sagittal section **(g)**, overgrowth of the right cerebellar hemisphere **(h)**, right posterior ventricle enlargement, small frontal horn, increased white matter volume and thickened cortical mantle **(i)**. **(j-l)** P01. Thickened corpus callosum **(j)**, with symmetrical enlargement of cerebellar **(k)** and cerebral hemispheres **(l)**.

Figure 3. Microscopy of paraffin embedded skin biopsies. (a) Numbers of melanocytes per field on whole skin sections from patients P05, P06 and P12 (patients: 6 fields; controls: 13 and 24 fields); hematoxylin eosin (HE) staining). DS = Dark skin; LS = light skin. **(b)** HE staining from P06 hypomelanotic skin. **(c)** Subject P12. Melan-A immunohistochemistry on skin biopsy sections from pigmented skin (top) and hypomelanotic skin (bottom). (d) Subject P12. MITF labeling on biopsy sections from pigmented skin (top) and hypomelanotic skin (bottom). Scale bar: 100 µm. Melanocytes are shown by arrowheads.

Figure 4. Ultrastructural study. (a) Melanosome maturation in melanocytes: Melanosome count in melanocytes on skin biopsy sections from pigmented (black) and hypopigmented area (white) in patients P12 (left) and P11 (right). Melanosomes were counted in 15 melanocytes. Upper bars: stage I melanosome. Lower bars: stage IV melanosomes (numbers at top of each bar). Ratio and total number of counted melanosomes are given at top and bottom of each figure. **(b) Melanosome quantification in keratinocytes.** Mean number of melanosomes per basal layer keratinocyte (n=50) **(c) TEM of melanocytes at the basal epidermal layer in subjects P12 (a, b) and P11 (c, d).** Melanosomes (arrows), in dark (a-c) and hypopigmented (b-d) areas. DS: Dark skin; LS: Light skin.

Figure 5. Clinical features in HI individuals with *MTOR* postzygotic pathogenic variants. (a) Frequencies of neurological involvement and overgrowth. **(b)** Standard deviations for OFC (dark grey) and body height (light grey). **(c)** Frequencies of recurrent facial features. Percentages were calculated with the number of patients with available data as the denominator. MI: Mild; MO: Moderate; S: Severe; ID: Intellectual disability.

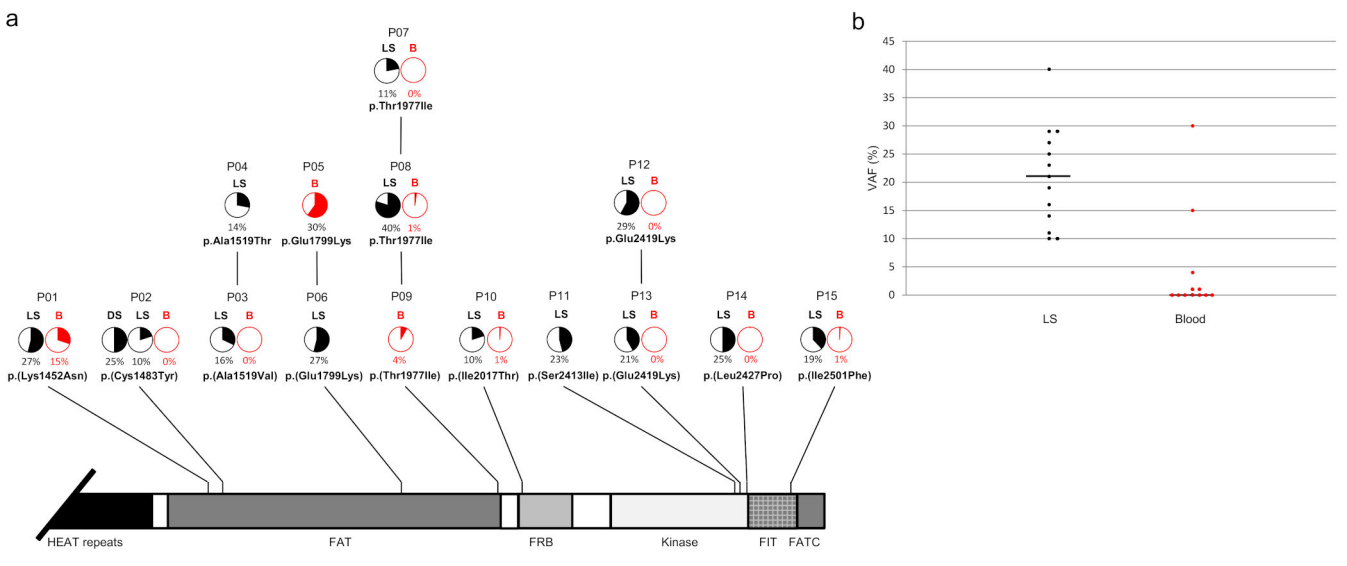
a
P07
LS B
11% 0%
p.Thr1977Ile
P04
LS
14%
p.Ala1519Thr
P05
B
30%
p.Glu1799Lys
P08
LS B
40% 1%
p.Thr1977Ile
P12
LS B
29% 0%
p.Glu2419Lys
P01
LS B
27% 15%
p.(Lys1452Asn)
P02
DS LS B
25% 10% 0%
p.(Cys1483Tyr)
P03
LS B
16% 0%
p.(Ala1519Val)
P06
LS
27%
p.(Glu1799Lys)
P09
B
4%
p.(Thr1977Ile)
P10
LS B
10% 1%
p.(Ile2017Thr)
P11
LS
23%
p.(Ser2413Ile)
P13
LS B
21% 0%
p.(Glu2419Lys)
P14
LS B
25% 0%
p.(Leu2427Pro)
P15
LS B
19% 1%
p.(Ile2501Phe)
HEAT repeats
FAT
FRB
Kinase
FIT
FATC
b
VAF (%)
45
40
35
30
25
20
15
10
5
0
LS
Blood

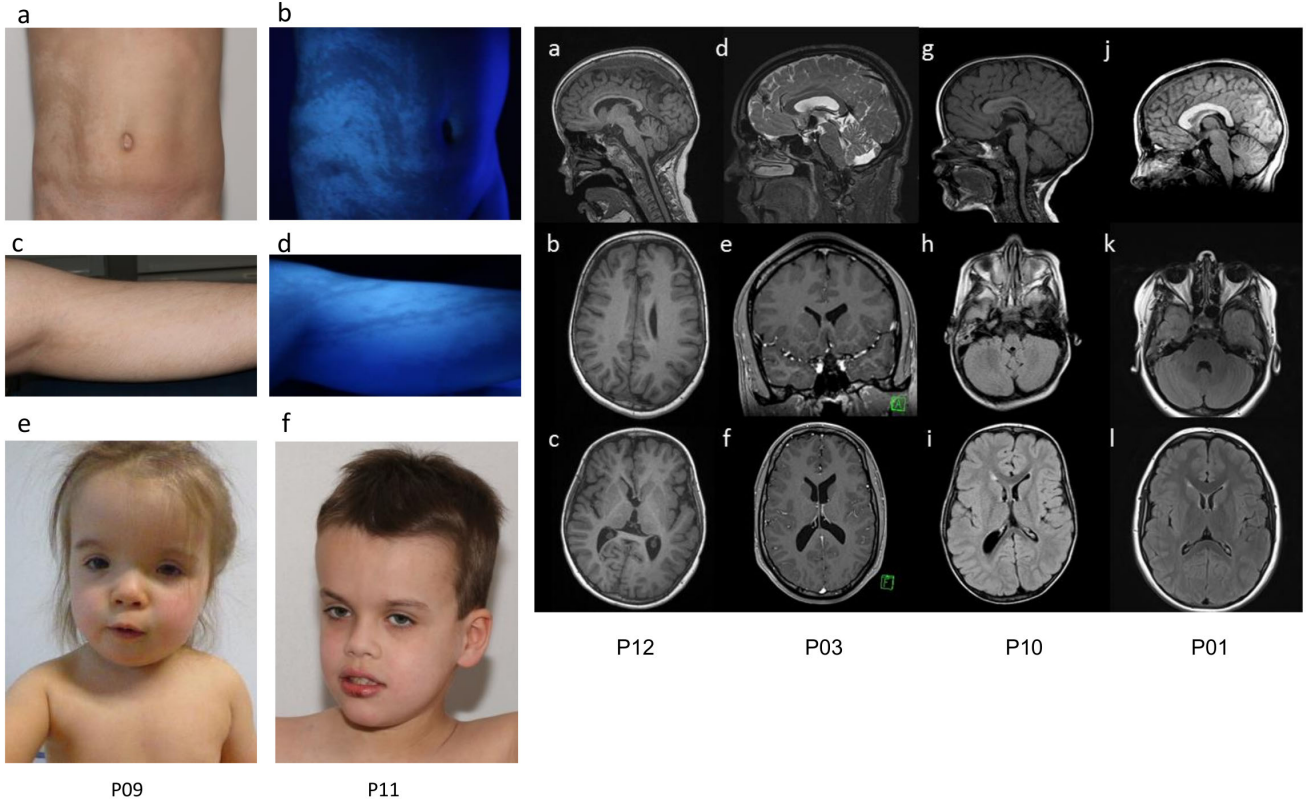
a
b
P11
c
d
P12
e
f
P09
P11
a
d
g
j
b
e
h
k
c
f
i
l
P12
P03
P10
P01

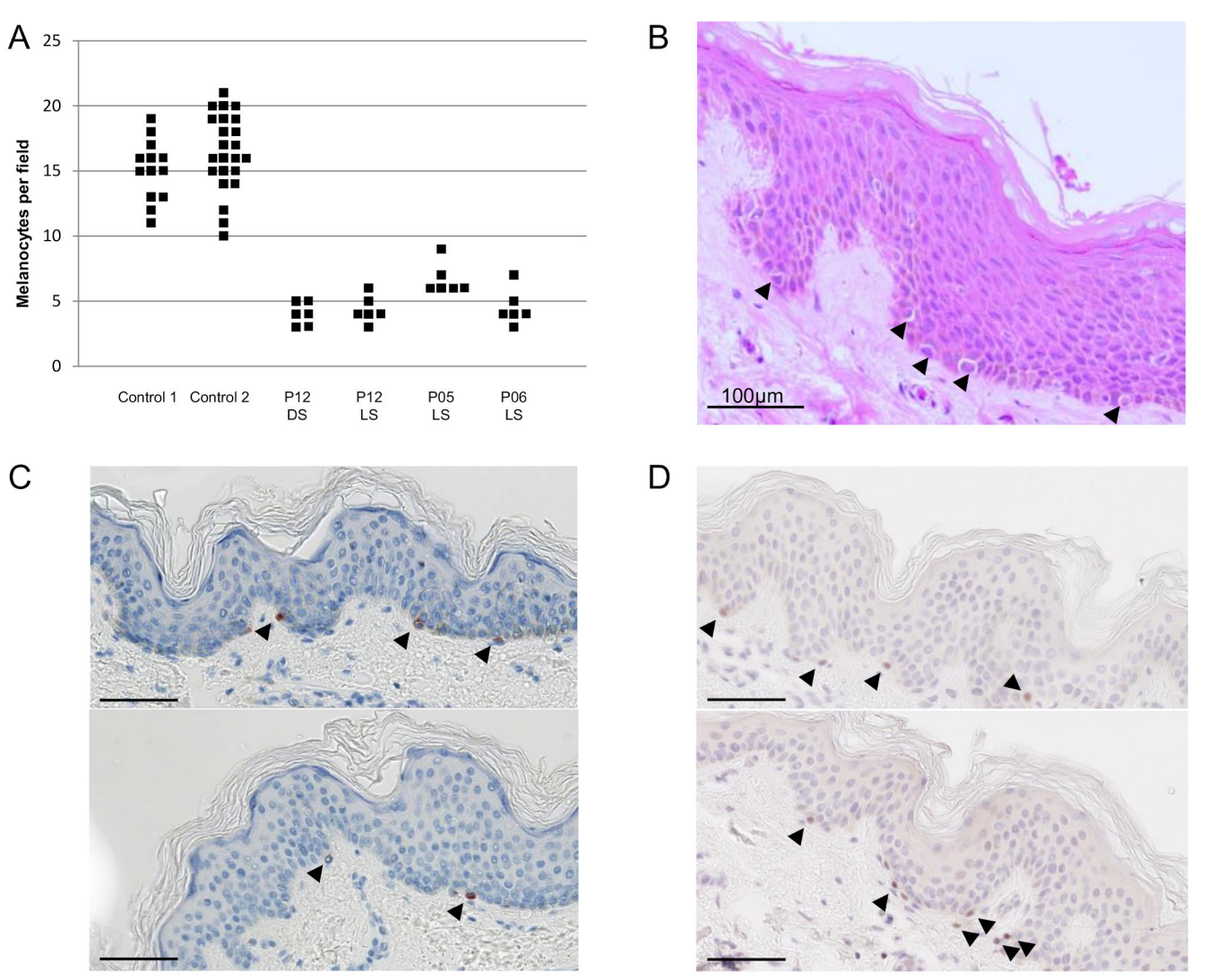
A
25
20
15
10
5
0
Melanocytes per field
Control 1
Control 2
P12 DS
P12 LS
P05 LS
P06 LS
B
100µm
C
D

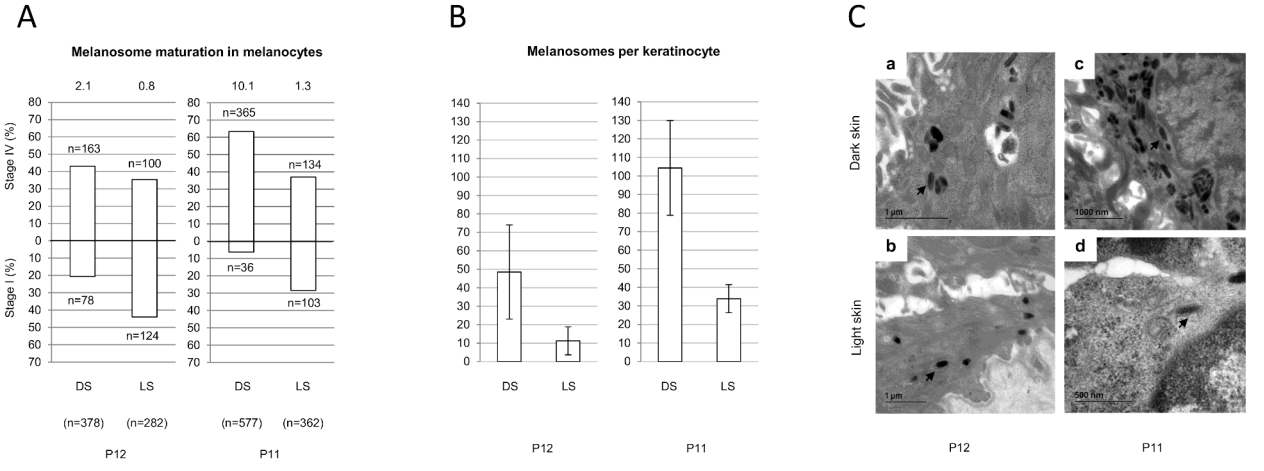
A
Melanosome maturation in melanocytes
2.1
0.8
10.1
1.3
Stage IV (%)
Stage I (%)
n=163
n=100
n=365
n=134
n=36
n=78
n=103
n=124
DS
LS
DS
LS
(n=378)
(n=282)
(n=577)
(n=362)
P12
P11
B
Melanosomes per keratinocyte
DS
LS
DS
LS
P12
P11
C
a
c
b
d
Dark skin
Light skin
1 µm
1000 nm
1 µm
500 nm
P12
P11

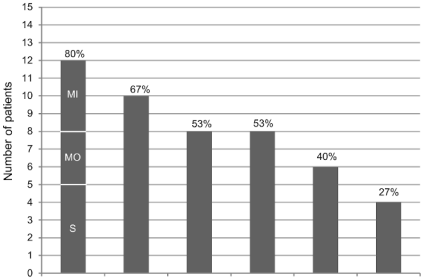
A
Number of patients
80%
67%
53%
53%
40%
27%
MI
MO
S
ID
Epilepsy
Macrocephaly z+3DS
HMEG/MEG
Unilateral overgrowth
ASD

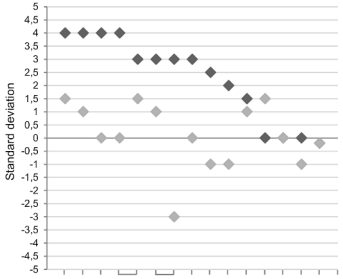
B
Standard deviation
p.Ile2017Thr
p.Lys1452Asn
p.Ser2413Ile
p.Glu1739Lys
p.Thr1977Ile
p.Ala1516Val
p.Cys1483Tyr
p.Ile2501Phe
p.Glu2419Lys
p.Leu2427Pro
p.Thr1977Ile
p.Ala1516Thr

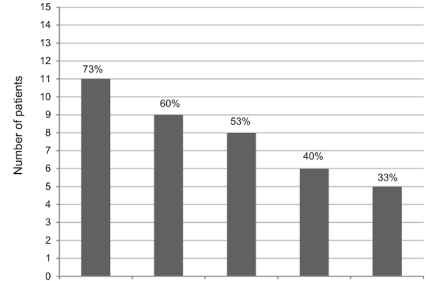
C
Number of patients
73%
60%
53%
40%
33%
High forehead
Hypertelorism
Depressed nasal bridge
Downslanting palpebral fissures
Anteverted nares

SUPPLEMENTARY MATERIAL

Supplementary Method

DNA Analysis

Exome capture and sequencing were performed at the Centre National de Génotypage (CNG, Evry, France) from 3 μg of genomic DNA for each patient sample. As a first approach, we performed deep exome sequencing on skin-derived and blood-derived DNA from 31 patients with pigmentary skin mosaicism, and blood from their parents. In subject P12, exome sequencing was performed on DNA obtained from a hypopigmented skin band (mean depth 200X), and blood-derived DNA from her unaffected parents (mean depth 80X). Data were processed as previously described [1]. Variant locations are based on the human genome reference sequence GRCh37/hg19. The Genome Analysis Toolkit (GATK) v.2.6-4 was used for base quality score recalibration, indel realignment, and variant discovery [2]. Candidate *de novo* events were systematically identified by focusing on protein-altering and splice-site variants. We assessed the presence of the identified variants in public variant databases, namely the Genome Aggregation Database (gnomAD, http://gnomad.broadinstitute.org/) and the Catalogue of somatic variants in cancer (COSMIC, http://cancer.sanger.ac.uk/cancergenome/projects/cosmic/).

Targeted deep sequencing was performed on all 57 coding regions of *MTOR* (reference accession LRG_734_t1). Sequences were amplified using custom intronic primers (sequences available on demand) and standard long-range PCR protocols. Libraries were prepared using the transposase-based Nextera XT DNA Sample Preparation kit (Illumina, Evry, France), and sequenced on a MiSeq instrument (Illumina, Evry, France) according to the manufacturer's recommendations.

Nucleotide-level conservation and impact of amino acid substitutions were assessed using Genomic Evolutionary Rate Profiling (GERP), Polyphen-2 (HumVar-trained model), and Combined Annotation-Dependent Depletion (CADD) scores. All prediction scores are listed in Supplementary Table 3.

Exome and targeted deep sequencing were performed according to standard protocol (detailed in Supplementary data). All MTOR variants identified were submitted to the CLINVAR database under

the number SUB8228199.

Supplementary Table 1. Previously reported *MTOR* variants in affected individuals with pigmentary features.

***MTOR* variant Amino acid change**	**Type of variant**	**Amino acid change***	**Available clinical features**	**References**
chr1:g.11217231A>G	Somatic	p.(Cys1483Arg)	Hemimegalencephaly, **hypomelanosis of Ito**	Lee JH *et al* 2012 [3]
	Somatic		Macrocephaly, ID, facial dysmorphism, **linear hyperpigmentation**	Gordo G *et al*, 2018 [4]
chr1:g.11188164G>T	Somatic	p.(Thr1977Lys)	Three unrelated patients with diffuse asymmetric MEG and **hypomelanosis of Ito**	Mirzaa GM *et al*, 2016 [5]
	Somatic		One patient with MEG, asymmetric polymicrogyria, hypotonia, and **hyperpigmentation**	Handoko M *et al*, 2019 [6]
chr1:g.11184612T>G	Germline	p.(Phe2202Cys)	Two siblings with macrocephaly, severe ID, capillary malformations (face and shoulder) and **area of hypo/hyperpigmentation**	Gordo G *et al*, 2018 [4]
chr1:g.11184573G>A	Somatic	p.(Ser2215Phe)	One patient with HMEG, severe ID, seizures, **hypochromic patches**	Pelorosso C *et al*, 2019 [7]

*Variant locations are based on GRCh37/hg19 and reference *MTOR* accession LRG_734_t1.

MEG: megalencephaly; FCD: Focal Cortical Dysplasia; ID: Intellectual Disability; HMEG::hemimegalencephaly.

Supplementary Table 2. Summary of exome sequencing experiments in subject PED1004 and her unaffected parents

Individual	DNA source	Target size (Mb)[a]	Aligned bases (Gb)[b]	Mean sequencing depth[c]	Percent target ≥ 10x[c]	Percent target ≥ 100x[c]
PED1004	Skin biopsy	51	20.798	242	96.5	81.6
Father	Blood	51	9.498	130	96.0	56.5
Mother	Blood	51	7.035	91	95.2	37.5

Mb, megabases; Gb, gigabases. [a]Target size of the SureSelect Human All Exon V5 kit (Agilent). [b]Bases from "P*assing Filter" (PF) reads* mapped to the human genome reference sequence (GRCh37/hg19 build of UCSC Genome Browser, see http://genome.ucsc.edu/). [c]Sequencing depth metrics were calculated using RefSeq coding exons and splice junctions as targets. Only reads with mapping quality ≥ 20 and bases with base quality ≥ 20 were considered.

Supplementary Table 3. Summary of mosaic *MTOR* changes

Subject	*MTOR* change	COSMIC ID	Gnomad allele frequency	GERP	Polyphen-2	CADD
P01	chr1:g.11217322T>A c.4356A>T p.(Lys1452Asn)	COSM462620	0/246,180	4.66	0.95	18.85
P02	chr1:g.11217230C>T c.4448G>A p.(Cys1483Tyr)	COSM462615	0/246,180	5.32	0.99	26.10
P03	chr1:g.11210197G>A c.4556C>T p.(Ala1519Thr)	COSM462614	0/246,138	5.16	0.98	34.00
P04	chr1:g.11210198C>T c.4555G>A p.(Ala1519Val)	COSM462614	0/246,138	5.16	0.997	22.5
P05 P06	chr1:g.11190804C>T c.5395G>A p.(Glu1799Lys)	COSM180789	0/246,180	5.54	0.878	26.3
P07 P08 P09	chr1:g.11188164G>A c.5930C>T p.(Thr1977Ile)	COSM6241477	0/246,096	3.73	0.96	9.68
P10	chr1:g.11187847A>G c.6050T>C p.(Ile2017Thr)	-	0/246,180	5.80	0.99	24.00
P11	chr1:g.11174437C>A c.7238G>T p.(Ser2413Ile)	COSM4703642	0/246,180	5.89	1.00	32.00
P12 P13	chr1:g.11174420C>T c.7255G>A p.(Glu2419Lys)	COSM4187184	0/246,028	5.89	1.00	36.00
P14	chr1:g.11174395A>G c.7280T>C p.(Leu2427Pro)	COSM5044474	0/246,180	5.89	1.00	26.00
P15	chr1:g.11169374T>A c.7501A>T p.(Ile2501Phe)	COSM4140746	0/246,180	5.82	0.99	21.60

CADD, Combined Annotation-Dependent Depletion; COSMIC, Catalogue of somatic mutations in cancer; Gnomad: Genome Aggregation Database; GERP, Genomic Evolutionary Rate Profiling [20–22].

Presence of identified *MTOR* variants was assessed in several public variant databases, including dbSNP build 141, Gnomad Browser, and COSMIC. All variants were absent from dbSNP build 14, and Gnomad database. Variant locations are based the human genome reference sequence GRCh37/hg19 and reference *MTOR* accession is LRG_734_t1.

Supplementary Table 4 : Phenotype and genotype of the fifteen affected individuals with *MTOR* variants.

Patient ID		P01	P02	P03	P04	P05	P06	P07	P08	P09	P10	P11	P12	P13	P14	P15
Age* (Y)		12	3	27	7	3	6	9	4	2.5	2.5	7	14	5.5	1	30
Sex		F	M	M	M	F	F	F	F	F	M	M	F	F	F	F
Hypomelanosis		Linear Trunk (P) (R), lower limbs	Linear R side	Linear Upper limb (L)	Linear Lower limb (L + R)	Linear Diffuse (trunk, upper + lower limbs)	Linear Diffuse (upper + lower limbs), trunk	Linear Lower limbs (R)	Linear Trunk (P), upper + lower limbs (L + R)	Linear Trunk, (P), limbs	Flag-like Upper limb (L), scalp hair patch (R)	Linear Trunk, back, groin (R)	Linear Trunk (A), Lower +, upper limbs (L)	Linear Trunk (R)	Linear Arm, Trunk (A) (R)	Linear Trunk, back, limbs (L)
Iris heterochromia		-	-	-	-	-	-	-	-	-	+	-	-	-	-	+
Unilateral overgrowth		Lower limbs	R	-	-	-	-	-	Lower limbs	R	Lower limbs	-	L	-	-	-
Macrocephaly		+	+	+	-	+	+	-	+	+	+	+	-	-	-	+
Neurodevelopmental disorder	ID	+	+	++	-	-	++	-	+++	+	++	+++	+++	+++	+	+++
	ASD	-	-	-	-	-	-	-	+	-	-	-	+	+	-	+
	Epilepsy	-	+	+	+	-	-	+	-	-	+	+	+	+	+	+
Brain MRI	Phenotype	MEG	HMEG (R)	HMEG (R)	NA	N	N	NA	NA	MEG	HMEG (R)	Mild HMEG (R)	HMEG (L)	NA	HMEG (R)	NA
	Asymmetry of LV	- (narrow FH of both LV)	Narrow FH of R LV	Narrow FH of R LV		-	-			-	Narrow FH of R LV	-	Narrow FH of L LV, enlarged L thalami and caudate nuclei	-		
	Corpus callosum	Globally thick	Asymmetry (R thicker + shorter)	Asymmetry (R shorter)		N	N			N	N	N	Asymmetry (L thicker)	Mild asymmetry		
	WM volume	Increased (both hemispheres)	N	Increased (R)		N	N			N	Increased (R)	Increased (R)	Increased (L)		Increased (R)	
	WM signal	N	N	N		N	N			N	N	Bilateral frontal neuronal heterotopias	N		N	
	Cerebral cortex	N	N	N		N	N			N	Thick (R)	N	L thick cortical mantle	N		
	Cerebellar hemispheres	N	Asymmetry (R>L)	N		N	N			N	Asymmetry (R>L)	N	Asymmetry (L>R)		Asymmetry (R>L)	
Psychomotor impairment		+	+++	+	-	-	++	-	+++	+	+	++	+++	++	++	+
Distal joint hyperlaxity		-	-	+	+	-	+	-	-	+	-	+	+	-	-	-
Hypertelorism		+	+	+	+	-	-	-	-	+	-	+	+	+	+	-
Downslanting palpebral fissures		+	-	-	+	+	-	-	+	+	-	-	-	-	+	-
Depressed nasal bridge		+	+	-	-	+	+	-	+	+	-	+	-	-	+	-
Scalp hair		Woolly	Curly	-	-	-	-	-	-	-	-	-	-	Sparse	Woolly	-
Anteverted nares		+	-	-	+	-	-	-	+	+	-	-	+	-	-	-
Teeth malposition		-	-	-	-	-	-	-	-	-	-	+	+	-	-	+
High forehead		-	+	+	+	-	-	+	+	+	+	+	+	+	+	-
Frontal bossing		-	+	-	-	-	-	-	+	+	-	+	-	+	-	-
Other features		Low hair line, microstomia	Thick upper lip, epicanthus	Synophris, low hair line, dysplastic ears	Long philtrum, thin upper lip	Sandal gap	Facial asymetry	-	Telecantus epicanthus	-	-	Thick upper lip, high-arched palate	-	-	-	-
Ocular anomalies		ND	Suspected	S	H	-	-	-	S, H, amblyopia	A, myopia	Coloboma	ND	RP	-	-	Left partial cataract
MTOR variant		p.(Lys1452Asn)	p.(Cys1483Tyr)	p.(Ala1519Val)	p.(Ala1519Thr)	p.(Glu1799Lys)	p.(Glu1799Lys)	p.(Thr1977Ile)	p.(Thr1977Ile)	p.(Thr1977Ile)	p.(Ile2017Thr)	p.(Ser2413Ile)	p.(Glu2419Lys)	p.(Glu2419Lys)	p.(Leu2427Pro)	p.(Ile2501Phe)
VAF (HI)		27%	10%	16%	14%	ND	27%	11%	40%	ND	10%	23%	29%	21%	25%	19%
VAF (Blood)		15%	-	-	ND	30%	ND	-	1%	4%	1%	-	-	-	-	-

* :at last examination, Y: year, ID: intellectual disability, ASD: autistic spectrum disorder; MEG:megalencephaly; HMEG:hemimegalencephaly; WM: white matter; ND: not determined; FH: Frontal horn; R: right-sided; L: left-

sided; A: anterior; P: posterior; +: presence; -: absence. ND : not determined ; S: strabismus; H: hypermetropia; As:astigmatism; RP: Retinitis pigmentosa

Supplementary Table 5 . Reports of individuals with hypomelanosis of Ito and hemimegalencephaly

Report	Linear hypo-pigmentation	Brain MRI findings	Seizures	Psychomotor delay or ID	Body hemi-hypertrophy	Ocular anomalies	Other features
(Peserico et al. 1988)[8]	+	HMEG, LV abnormal shape	+	+	-	Divergent strabismus	-
(Battistella et al. 1990)[9]	+	HMEG, LV abnormal shape, abnormal periventricular WM signal	+	+	-	Divergent strabismus hypo-pigmented iris	-
(Battistella et al. 1990)[9]	+	HMEG, abnormal periventricular WM signal	-	-	-	Divergent strabismus	Facial dysmorphism, dysondotiasis
(Williams and Elster 1990)[10]	+	HMEG, abnormal periventricular WM signal	-	+	+	Optic nerve abnormality, retinal detachment, cataract	Imperforate anus, colon atresia, syndactyly clinodactyly, cleft palate, bilateral conductive hearing loss, facial asymmetry, dental anomalies
(Malherbe et al. 1993)[11]	+	HMEG, enlarged LV, pachygyria, poor delineation grey-WM	+	+	-	-	-
(Tagawa et al. 1994)[12]	+	HMEG, cortical thickening, pachygyria, LV abnormal shape, poor delineation grey-WM	+	-	-	Hypo-pigmented iris	-
(Steiner et al. 1996)[13]	+	HMEG, LV abnormal shape, poor delineation grey-WM	+	+	-	-	Hemiparesis
(Auriemma et al. 2000)[14]	+	HMEG, cortical thickening, pachygyria, LV abnormal shape	+	Unknown	+	-	Hypotonia
(Chapman and Cardenas 2008)[15]	+	HMEG	+	+	-	-	-
(Sharma et al. 2009)[16]	+	HMEG, cortical thickening	+	+	+	-	-
(Assogba et al. 2010)[17]	+	HMEG, calcifications in caudate and lentiformis nuclei	+	+	+	-	Mild liver enlargement
(Lee and al, 2012)[3]	+	HMEG, cortical dysplasia, ectopic and cytomegalic neurons	-	Unknown	Unknown	Unknown	Unknown
(Okanari et al. 2014)[18]	+	HMEG, right FCD, enlargement right cerebral hemisphere	+	+	-	Unknown	Hypotonia
(Cuddapah et al, 2015)[19]	+	HMEG, unilateral enlargement of left parietal and occipital lobe	+	+	-	-	-
(Pelorosso et al. 2019)[7]	+	HMEG, enlarged ventricles, brain midline rightward deviation, cortical thickening, abnormal WM signal	+	+	-	-	-

HMEG, hemimegalencephaly; MRI, Magnetic resonance imaging; ID, intellectual disability; WM, white matter; LV: Lateral ventricule.; FCD: focal cortical dysplasia.

SUPPLEMENTARY FIGURES

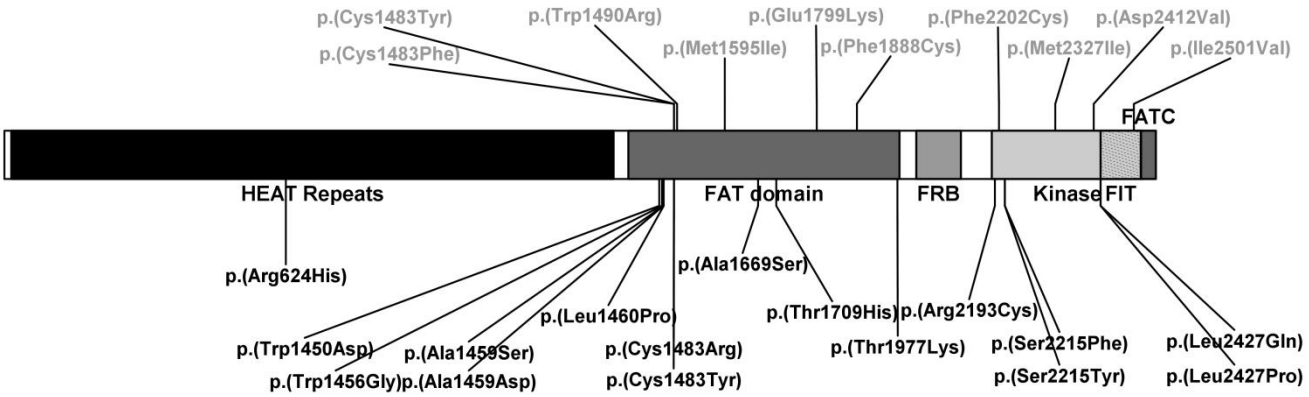

Supplementary Figure 1. Schematic representation of MTOR protein structure with previously reported germinal (light gray) and somatic variants (black)[3–7,23–29]**.** FAT: FRAP-ATM-TRRAP domain ; FRB : FKBP12-Rapamycin Binding domain ; FATC: C-terminal FAT domain.

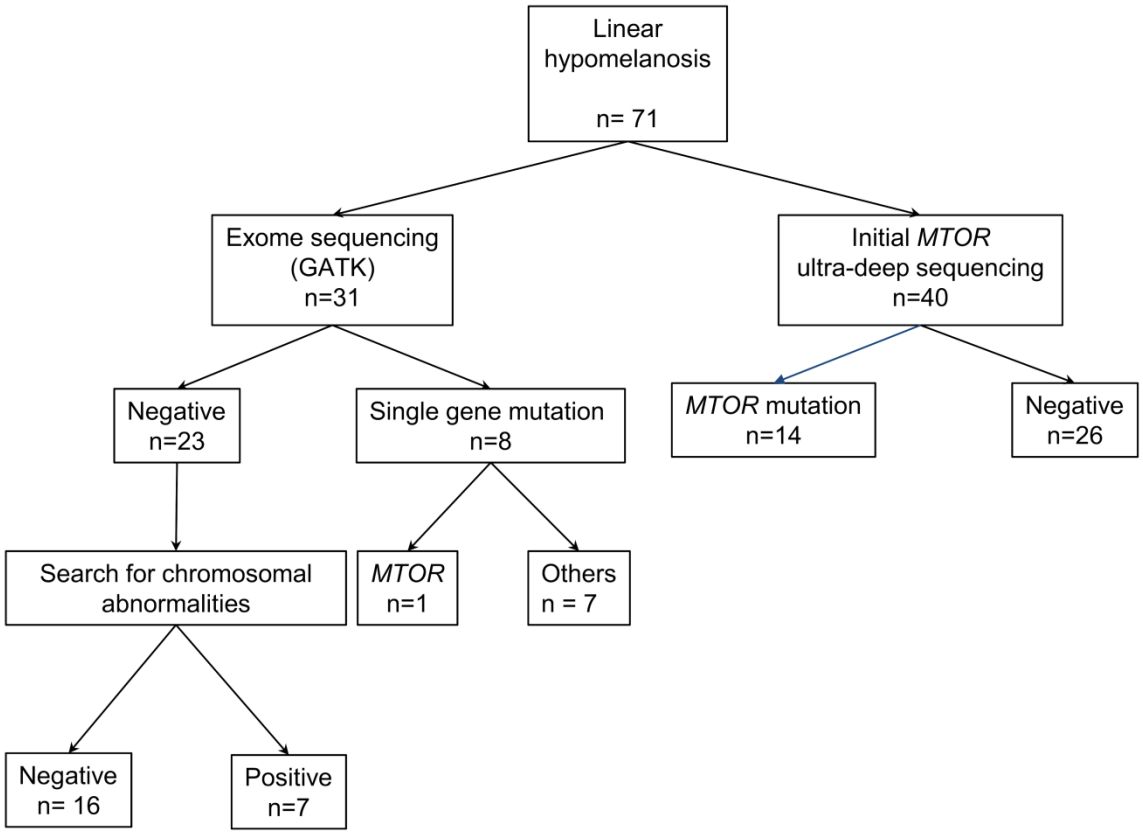

Supplementary Figure 2. Next generation sequencing approach in patients with hypomelanosis of Ito.

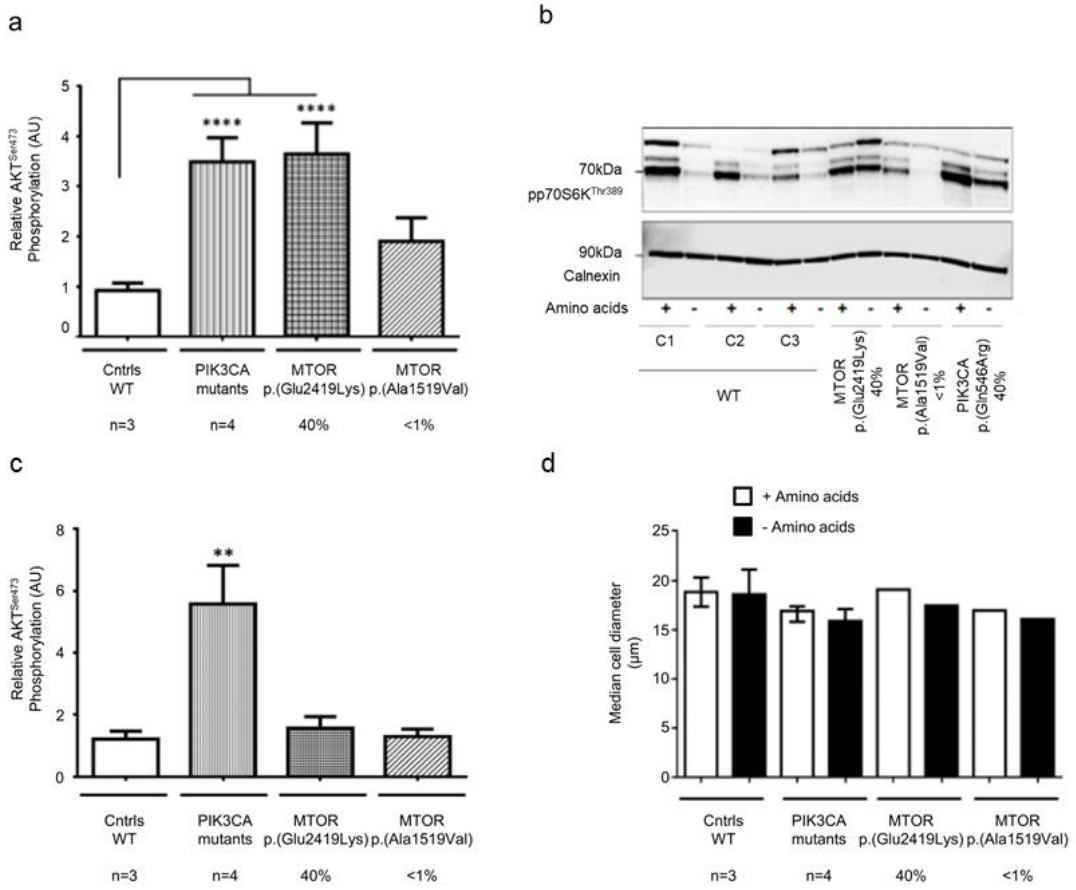

Supplementary Figure 3. Evaluation of AKT^{ser473} and p70S6K^{thr389} phosphorylation in *MTOR* mutant cell lines following amino acid deprivation (a-b), without amino acid deprivation (c) and cell size in *MTOR* mutant cell lines (d). (a) ELISA based evaluation of AKT^{ser473} phosphorylation following 50 minutes of amino acid deprivation in wild type control dermal fibroblasts (Cntrls, n=3), *PIK3CA* mutant fibroblast cell lines (n=4 with respective variant allele fractions; M020 [p.(Gly1049Arg) / 40%], M098 [p.(Glu418Lys) / 32%], M018 [p.(Gln546Lys) / 40%] and M032 [p.(His1047Arg) / 30%]) and *MTOR* mutant fibroblast cell lines p.(Glu2419Lys) (VAF = 40%) and p.(Ala1519Lys) (VAF < 1%). Skin fibroblasts from patients with *PIK3CA* variants were used as positive controls. Data is pooled from three independent experiments and error bars represent standard error of the mean (SEM). **** $p < 0.0001$ One-way ANOVA, Tukey's post-hoc analyses. **(b)** Western blot of p70S6K phosphorylation with or without 50 minutes of amino acid deprivation of control wild type cells (C1-C3), a *PIK3CA* mutant cell line (M18, p.(Gln546Lys) 40%) and two

MTOR mutant cell lines (p.(Glu2419Lys) and p.(Ala1519Val)). Representative of four independent experiments; calnexin has been used as a loading control. **(c)** ELISA based evaluation of AKT^{ser473} phosphorylation without amino acid deprivation in wild type control cells (Cntrls, n=3), *PIK3CA* mutant cell lines (n=4 with respective pathogenic variation burdens; M020 [p.(Gly1049Arg) 40%], M098 [p.(Glu418Lys) 32%], M018 [p.(Gln546Lys) 40%] and M032 [p.(His1047Arg) 30%]) and *MTOR* mutant cell lines p.(Glu2419Lys) (40% pathogenic variation burden) and p.(Ala1519Lys) (<1% pathogenic variation burden). Data is pooled from three independent experiments and error bars represent SEM. **p < 0.01 One-way ANOVA, Tukey's post-hoc analyses. **(d)** Median cell diameter using a FACS-based multi-sizer with or without amino acid deprivation for 50 minutes. Pathogenic variation burdens are indicated below. Error bars represent SEM; 10,000 cells were counted in total. Skin fibroblasts from patients with known activating *PIK3CA* variants were used as positive controls and cultured primary fibroblasts carrying p.(Ala1519Val) pathogenic variation were used for comparison.

Supplementary bibliography

1. Sorlin A, Maruani A, Aubriot-Lorton M-H, et al. Mosaicism for a KITLG Mutation in Linear and Whorled Nevoid Hypermelanosis. *Journal of Investigative Dermatology*. 2017;137(7):1575-1578.

2. DePristo MA, Banks E, Poplin RE, et al. A framework for variation discovery and genotyping using next-generation DNA sequencing data. *Nat Genet*. 2011;43(5):491-498.

3. Lee JH, Huynh M, Silhavy JL, et al. De novo somatic mutations in components of the PI3K-AKT3-mTOR pathway cause hemimegalencephaly. *Nat Genet*. 2012;44(8):941-945.

4. Gordo G, Tenorio J, Arias P, et al. mTOR mutations in Smith-Kingsmore syndrome: Four additional patients and a review. *Clinical Genetics*. 2018;93(4):762-775.

5. Mirzaa GM, Campbell CD, Solovieff N, et al. Wide spectrum of developmental brain disorders from megalencephaly to focal cortical dysplasia and pigmentary mosaicism caused by mutations of MTOR. *JAMA Neurol*. 2016;73(7):836-845.

6. Handoko M, Emrick LT, Rosenfeld JA, et al. Recurrent mosaic MTOR c.5930C > T (p.Thr1977Ile) variant causing megalencephaly, asymmetric polymicrogyria, and cutaneous pigmentary mosaicism: Case report and review of the literature. *Am J Med Genet A*. 2019;179(3):475-479.

7. Pelorosso C, Watrin F, Conti V, et al. Somatic double-hit in MTOR and RPS6 in hemimegalencephaly with intractable epilepsy. *Hum Mol Genet*. Published online August 14, 2019.

8. Peserico A, Battistella PA, Bertoli P, Drigo P. Unilateral Hypomelanosis of Ito with Hemimegalencephaly. *Acta Paediatrica*. 1988;77(3):446-447.

9. Battistella PA, Peserico A, Bertoli P, Drigo P, Laverda AM, Casara GL. Hypomelanosis of Ito and hemimegalencephaly. *Childs Nerv Syst*. 1990;6(7):421-423.

10. Williams DW, Elster AD. Cranial MR imaging in hypomelanosis of Ito. *J Comput Assist Tomogr*. 1990;14(6):981-983.

11. Malherbe V, Pariente D, Tardieu M, et al. Central nervous system lesions in hypomelanosis of Ito: an MRI and pathological study. *J Neurol*. 1993;240(5):302-304.

12. Tagawa T, Otani K, Futagi Y, et al. [Hypomelanosis of Ito associated with hemimegalencephaly]. *No To Hattatsu*. 1994;26(6):518-521.

13. Steiner J, Adamsbaum C, Desguerres I, et al. Hypomelanosis of Ito and brain abnormalities: MRI findings and literature review. *Pediatr Radiol*. 1996;26(11):763-768.

14. Auriemma A, Agostinis C, Bianchi P, et al. Hemimegalencephaly in hypomelanosis of Ito: early sonographic pattern and peculiar MR findings in a newborn. *European Journal of Ultrasound*. 2000;12(1):61-67. d

15. Chapman K, Cardenas JF. Hemimegalencephaly in a Patient With a Neurocutaneous Syndrome. *Seminars in Pediatric Neurology*. 2008;15(4):190-193.

16. Sharma S, Sankhyan N, Kabra M, Kumar A. Hypomelanosis of Ito with hemimegalencephaly. *Dermatol Online J*. 2009;15(11):12.

17. Assogba K, Ferlazzo E, Striano P, et al. Heterogeneous seizure manifestations in Hypomelanosis of Ito: report of four new cases and review of the literature. *Neurological Sciences*. 2010;31(1):9-16.

18. Okanari K, Miyahara H, Itoh M, et al. Hemimegalencephaly in a Patient With Coexisting Trisomy 21 and Hypomelanosis of Ito. *J Child Neurol*. 2014;29(3):415-420.

19. Cuddapah VA, Thompson M, Blount J, Li R, Guleria S, Goyal M. Hemispherectomy for Hemimegalencephaly Due to Tuberous Sclerosis and a Review of the Literature. *Pediatric Neurology*. 2015;53(5):452-455.

20. Cooper GM, Stone EA, Asimenos G, Green ED, Batzoglou S, Sidow A. Distribution and intensity of constraint in mammalian genomic sequence. *Genome Res*. 2005;15(7):901-913.

21. Adzhubei IA, Schmidt S, Peshkin L, et al. A method and server for predicting damaging missense mutations. *Nat Methods*. 2010;7(4):248-249.

22. Kircher M, Witten DM, Jain P, O'Roak BJ, Cooper GM, Shendure J. A general framework for estimating the relative pathogenicity of human genetic variants. *Nat Genet*. 2014;46(3):310-315.

23. EPI4K Consortium, Epilepsy Phenome/Genome project. De novo mutations in the classic epileptic encephalopathies. *Nature*. 2013;501(7466):217-221.

24. Smith L, Saunders CJ, Dinwiddie DL, et al. Exome Sequencing Reveals De Novo Germline Mutation of the Mammalian Target of Rapamycin (MTOR) in a Patient with Megalencephaly and Intractable Seizures. *Journal of Genomes and Exomes*. 2013;2:63-72.

25. Baynam G, Overkov A, Davis M, et al. A germline MTOR mutation in Aboriginal Australian siblings with intellectual disability, dysmorphism, macrocephaly, and small thoraces. *American Journal of Medical Genetics Part A*. 2015;167(7):1659-1667.

26. D'Gama AM, Geng Y, Couto JA, et al. mTOR Pathway Mutations Cause Hemimegalencephaly and Focal Cortical Dysplasia. *Ann Neurol*. 2015;77(4):720-725.

27. Lim JS, Kim W, Kang H-C, et al. Brain somatic mutations in MTOR cause focal cortical dysplasia type II leading to intractable epilepsy. *Nature Medicine*. 2015;21(4):395-400.

28. Moosa S, Böhrer-Rabel H, Altmüller J, et al. Smith–Kingsmore syndrome: A third family with the MTOR mutation c.5395G>A p.(Glu1799Lys) and evidence for paternal gonadal mosaicism. *American Journal of Medical Genetics Part A*. 2017;173(1):264-267.

29. Rodríguez-García ME, Cotrina-Vinagre FJ, Bellusci M, et al. A novel de novo MTOR gain-of-function variant in a patient with Smith-Kingsmore syndrome and Antiphospholipid syndrome. *Eur J Hum Genet*. 2019;27(9):1369-1378.